ACS chemical biology

ARTICLE

Divergent Synthesis of Multifunctional Molecular Probes To Elucidate the Enzyme Specificity of Dipeptidic γ-Secretase Inhibitors

Haruhiko Fuwa[†,*], Yasuko Takahashi[‡], Yu Konno[†], Naoto Watanabe[‡], Hiroyuki Miyashita[‡], Makoto Sasaki[†], Hideaki Natsugari[¶,#], Toshiyuki Kan[$,§], Tohru Fukuyama[§], Taisuke Tomita[‡,*], and Takeshi Iwatsubo[‡]

[†]Laboratory of Biostructural Chemistry, Graduate School of Life Sciences, Tohoku University, 1-1 Tsutsumidori-Amamiya, Aoba-ku, Sendai 981-8555, Japan, [$]School of Pharmaceutical Sciences, University of Shizuoka, 52-1 Yada, Suruga-ku, Shizuoka 422-8526, Japan, [#]Laboratory of Synthetic Organic and Medicinal Chemistry, Faculty of Pharmaceutical Sciences, Teikyo University, Sagamiko, Tsukui-gun, Kanagawa 199-0195, Japan, [‡]Department of Neuropathology and Neuroscience, [¶]Laboratory of Rational Medicinal Science, and [§]Laboratory of Synthetic Natural Products Chemistry, Graduate School of Pharmaceutical Sciences, The University of Tokyo, 7-3-1 Hongo, Bunkyo-ku, Tokyo 113-0033, Japan

ABSTRACT Divergent synthesis of multifunctional molecular probes based on caprolactam-derived dipeptidic γ-secretase inhibitors (GSIs), Compound E (CE) and LY411575 analogue (DBZ), was efficiently accomplished by means of Cu(I)-catalyzed azide/alkyne fusion reaction. Photoaffinity labeling experiments using these derivatives coupled to photoactivatable and biotin moieties provided direct evidence that the molecular targets of CE and DBZ are the N-terminal fragment of presenilin 1 within the γ-secretase complex. Moreover, these photoprobes directly targeted signal peptide peptidase. These data suggest that the divergent synthesis of molecular probes has been successfully applied to characterize the interaction of GSIs with their molecular targets and define the structural requirements for inhibitor binding to intramembrane-cleaving proteases.

*Corresponding authors, hfuwa@bios.tohoku.ac.jp, taisuke@mol.f.u-tokyo.ac.jp.

Received for review April 3, 2007 and accepted April 25, 2007.

Published online May 25, 2007

10.1021/cb700073y CCC: $37.00

Alzheimer's disease (AD) is a neurodegenerative disorder and currently a serious public health problem in aging societies (*1*). AD is pathologically characterized by the extensive extracellular deposition of amyloid-β (Aβ) peptides as senile plaques in cerebral cortices. γ-Secretase is responsible for the proteolytic processing of amyloid precursor protein (APP) within the transmembrane domain to generate Aβ peptides. Thus, the inhibition of "amyloidogenic" APP processing by γ-secretase inhibitor (GSI) is one of the most important strategies toward the prevention and treatment of AD. γ-Secretase is a membrane-bound macromolecular complex composed of presenilin (PS) 1, presenilin enhancer 2 (Pen-2), anterior pharynx-defective 1 (Aph-1), and nicastrin. Importantly, γ-secretase cleaves not only APP but also several membrane proteins, including Notch receptors, which have been implicated in development, cell fate determination, and cancer biology (*2*). Moreover, much attention is now focused on the signal peptide peptidase (SPP) family, which belongs to the PS-type intramembrane cleaving aspartic protease family and shares the same consensus sequence at the catalytic site (*3*). SPP family proteins are also implicated in development, innate immunity, and infectious diseases (*4*–*8*). Thus, the temporal, spatial, and enzyme-specific control of these PS-type proteases by organic small molecules is now an important issue with regard to the understanding of the physiological function as well as the development of therapeutics against human diseases.

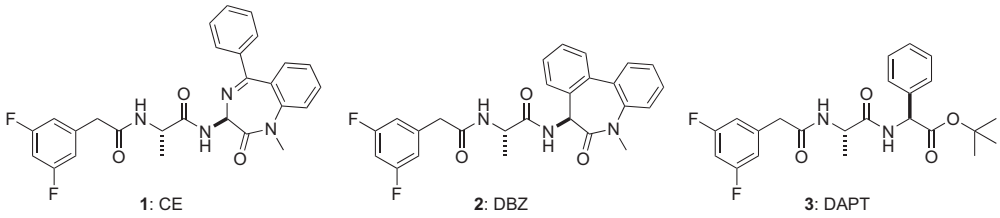

Figure 1. The structure of representative dipeptidic γ-secretase inhibitors.

To date, several GSIs have been reported and classified by their chemical structures (*1*). Among these, a dipeptidic class of GSI, such as benzodiazepine-type Compound E (**1**, CE), dibenzoazepine-type LY411575 analogue (**2**, DBZ), and (*N*-[*N*-(3,5-difluorophenylacetyl)-L-alanyl]-(*S*)-phenylglycine *tert*-butyl ester (**3**, DAPT), is known as one of the potent GSIs *in vitro* as well as *in vivo* (Figure 1). Of note, DAPT is reported as a γ-secretase-specific inhibitor, while LY411575 cross-inhibits a proteolytic activity of SPP *in vitro* as well as the cell-based assay (*9*–*11*). Since the first report by Seiffert *et al.* (*12*), several enzymological and chemical biological approaches have been utilized to define the target and mode of action of dipeptidic GSIs on γ-secretase (*e.g.*, photoaffinity labeling (*12, 13*), cross-competition (*14, 15*), and radioligand binding (*12, 14, 16*)). However, the molecular mechanisms whereby dipeptidic GSIs other than DAPT cross-inhibit SPP still remain unknown. Thus, the identification and the characterization of molecular targets/domains in γ-secretase and SPP of these representative dipeptidic GSIs would provide significant information on the structure and functions of these atypical proteases. A multifunctional probe harboring an affinity ligand, a photoactivatable group as cross-linking unit, and biotin as a reporter group should serve as powerful tools (*17*–*20*). We recently performed a systematic derivatization of DAPT and identified the C-terminal fragment (CTF) of PS1 as its molecular target, using a biotinylated photoaffinity probe DAP-BpB (*13, 21, 22*). Herein, we describe our divergent approach for the synthesis of multifunctional molecular probes of two highly potent caprolactam-derived dipeptidic GSIs, CE and DBZ, by means of the copper(I)-mediated azide/alkyne fusion process (*23, 24*).

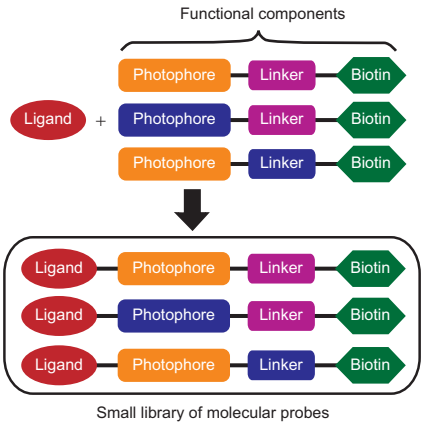

Figure 2. Strategy for divergent synthesis of multifunctional molecular probes.

RESULTS AND DISCUSSION

Chemistry and Synthesis. Elaboration of a structurally complex, biologically active small molecule into a multifunctional molecular probe involves two synthetically challenging tasks. First, it calls for careful synthetic planning that allows installation of functional components (*e.g.*, photophore and biotin-tag) in the presence of sensitive functional groups. Conventional strategies often involve amide bond-forming reactions, which generally require multistep synthetic manipulations accompanied with tedious purification steps. In particular, synthesis of biotinylated molecular probes is often problematic and laborious due to the difficulties in handling and purification of sparingly soluble biotin derivatives. For these reasons, it was envisaged that utilization of chemical "ligation" reactions as a means to introduce functional components would be ideal, in that they are generally highly chemoselective clean processes essentially devoid of side reactions (and thus product isolation is facile) and are tolerant of various solvents, including water and alcohols that are capable of dissolving biotin derivatives. A second challenge exists in design of a molecular probe that is truly effective for labeling and detection of a target biomolecule(s). Even if

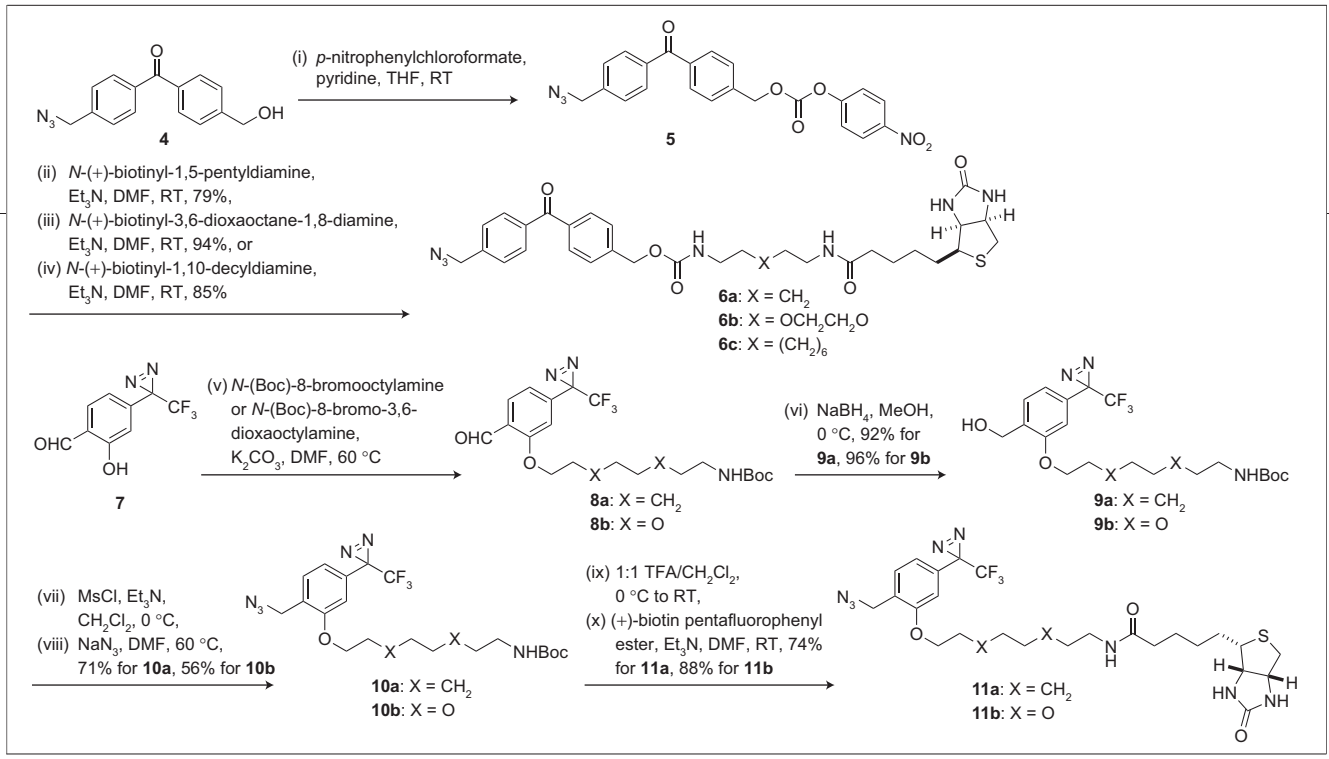

Scheme 1. Synthesis of benzophenone-type azides. Key: Boc = *tert*-butoxylcarbonyl; DMF = *N*,*N*′-dimethylformamide; Ms = methanesulfonyl; TFA = trifluoroacetic acid.

structure–activity relationships (SARs) of an affinity ligand moiety are provided, labeling ability of a designed molecular probe can only be evaluated experimentally; repetition of chemical synthesis and labeling experiments is often required. Therefore, synthesis and evaluation in a combinatorial fashion would be a powerful and efficient strategy for discovery of an effective molecular probe.

Toward realization of combinatorial synthesis and evaluation of multifunctional molecular probes, an efficient solid-phase methodology has been developed in our group (*21*). Complementary to this solid-phase chemistry, strategies utilizing chemoselective ligation reactions for coupling of a diverse set of functional components with an affinity ligand moiety would be particularly attractive as a solution-phase counterpart (Figure 2). Indeed, Hatanaka and co-workers (*25*) have successfully utilized the oxime ligation for one-step synthesis of biotinylated photoaffinity probes, although its application has been limited to unprotected sugars. On the other hand, the Cu(I)-mediated azide/alkyne fusion reaction was particularly attractive for us because it just requires functional handles (*i.e.*, azide and terminal alkyne) that are very easy to incorporate by standard organic synthesis and do not need protective group chemistry (*26, 27*). On the basis of our previous SAR analysis (*22*), we planned to synthesize five types of azides (**6a**–**c** and **11a,b**) and two types of alkynes (**17** and **19**) and unify each component by the azide/alkyne fusion process, thereby generating 10 types of molecular probes. In this way, solution-phase divergent synthesis of multifunctional molecular probes would be efficiently accomplished (*26, 27*).

Synthesis of the benzophenone-type azides, **6a**–**c**, was performed by the activation of the known alcohol **4** (*21*) with *p*-nitrophenyl chloroformate followed by coupling of the derived **5** with the appropriate biotinylated amines (Scheme 1). The phenyldiazirine-type azides, **11a**,**b**, were elaborated from the known alcohol **7** (*28*–*30*) (Scheme 1). Alkylation of **7** with the appropriate bromide (*31, 32*) followed by reduction of the derived aldehydes, **8a**,**b**, with sodium borohydride gave the alcohols **9a**,**b**, which was converted to the azides, **10a**,**b**, *via* mesylation and displacement with sodium azide. Removal of the *tert*-butoxycarbonyl (Boc) group and ensuing coupling with (+)-biotin pentafluorophenyl ester gave rise to the azides, **11a**,**b**. Although alkyl and ethylene glycol linkers were utilized in the present study, other linkers of different properties such as acid-, thiol-, or enzyme-cleavable may also be employed (*33*–*36*). Synthesis of the CE alkyne **17** was commenced with the known azide **12** (*37*) (Scheme 2). Treatment of **12** with triphenylphosphine in aqueous THF followed by *in situ* protection of the resultant amine with Boc_2O and subsequent deprotection of the *p*-methoxybenzyl group of the derived **13** by ceric ammonium nitrate at low temperature (CH_3CN/H_2O, −15 °C) provided the lactam **14** in 76% overall yield. Selective alkylation of the lactam nitrogen with propargyl bromide and cesium carbonate furnished **15** in 70% yield.

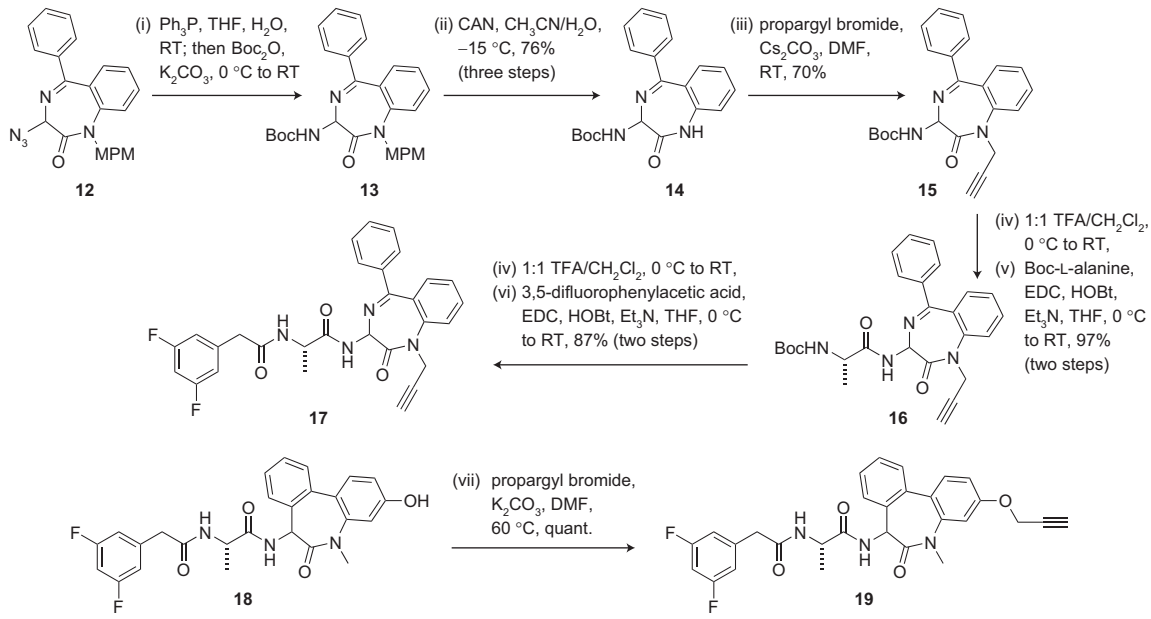

Scheme 2. Synthesis of CE alkyne 17**. Key: Boc = *tert*-butoxylcarbonyl; CAN = ceric ammonium nitrate; TFA = trifluoroacetic acid; EDC = 1-(3-(dimethylamino)propyl)-3-ethylcarbodiimide hydrochloride; HOBt = 1-hydroxybenzotriazole.**

Removal of the Boc group and the ensuing coupling with Boc-L-alanine afforded the product **16** (97% yield for the two steps), which was elaborated into the alkyne **17** by Boc deprotection and coupling with 3,5-difluorophenylacetic acid in 97% yield for the two steps. On the other hand, the DBZ alkyne **19** was prepared quantitatively by alkylation of our previously synthesized alcohol **18** (*38*) with propargyl bromide (Scheme 2)\.

With the requisite alkynes and azides in hand, we set out on the synthesis of multifunctional probes based on the copper(I)-mediated azide/alkyne fusion process. We first examined the reaction using the alkyne **17** and the azide **6a** in 1:1 stoichiometry as a model case (Table 1). Under the prototypical Sharpless conditions, the reaction proceeded very sluggishly and produced only a trace amount of the desired product **21a** (entry 1). When the reaction mixture was heated to 80 °C, the reaction completed within 3 d to give **21a** in 70% yield, but an unidentified side product that was difficult to separate from **21a** also formed (entry 2). In contrast, the addition of tris(triazolyl)amine, **20** (*39*), facilitated a clean reaction to provide the desired **21a** in 89% yield, although the reaction took 12 d at RT for completion (entry 3). The surprisingly low reactivity under the $CuSO_4$/sodium ascorbate catalytic system prompted us to further investigate the reaction conditions. We subsequently found that on using a catalytic amount of copper(I) iodide (CuI) in the presence of *N*,*N*-diisopropylethylamine (*i*-Pr_2NEt) in methanol, the reaction proceeded smoothly to give **21a** in 92% yield after 20 h at RT (entry 4). We observed no significant effect of the addition of **20** when used in combination with CuI (entry 5). Encouraged by these results, various substrate combinations were tested under aqueous and/or anhydrous conditions. In each case, the desired probe was generated in moderate to excellent yield, demonstrating that the present strategy is feasible for the synthesis of a diverse set of biotinylated photoaffinity probes (Table 2). In addition, the present results highlight the reactivity difference between two catalytic systems, $CuSO_4$/sodium ascorbate and CuI; the direct use of CuI accelerated the reaction, although in some cases the yields are somewhat moderate.

Biological Evaluation and Photoaffinity Labeling Experiments. Biological evaluation of the affinity probes thus obtained was performed by our cell-free *in vitro* assay using recombinant CTF of APP as a substrate (*40*). The affinity probes of the **21a–e** and **22a–e** displayed strong inhibitory potency against Aβ production compa-

TABLE 1. Cu(I)-catalyzed azide/alkyne cycloaddition reaction

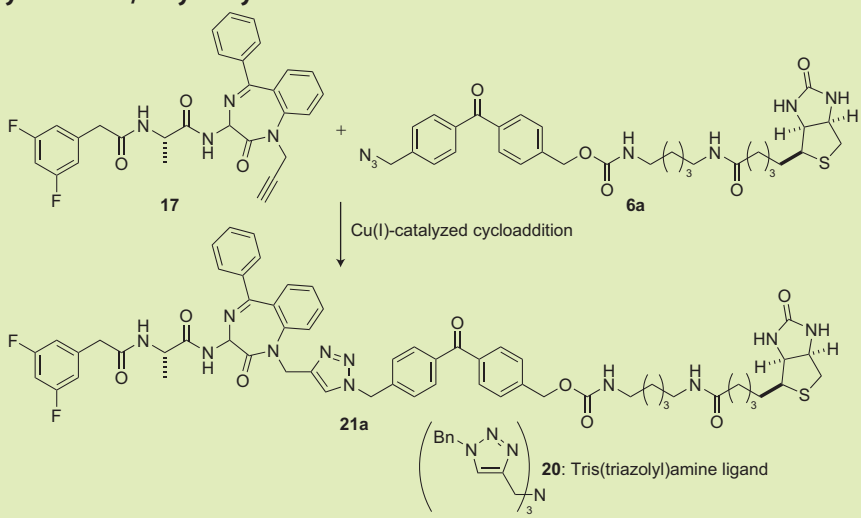

Entry	Reagents (equiv)	Solvent	Temp	Time	% yield
1	$CuSO_4$ (0.1), sodium ascorbate (0.2)	*t*-BuOH/H_2O (1:1)	RT	3 d	Trace
2	$CuSO_4$ (0.1), sodium ascorbate (0.2)	*t*-BuOH/H_2O (1:1)	80 °C	3 d	70
3	$CuSO_4$ (0.1), sodium ascorbate (0.2), **20** (0.4)	MeOH/H_2O (3:1)	RT	12 d	87
4	CuI (0.3), *i*-Pr_2NEt (10)	MeOH	RT	20 h	92
5	CuI (0.3), *i*-Pr_2NEt (10), **20** (0.3)	MeOH	RT	20 h	87

rable to that of the parental compounds (Table 2). These results suggested that these probes maintain sufficient affinity toward γ-secretase. Next, we performed the photoaffinity labeling experiments using **21a**–**e** and **22a**–**e**. We have previously found that a structural relative, DAP-BpB, directly bound to 23–26 kDa polypeptides that correspond to PS1 CTF (*13*). Unexpectedly, however, no photoaffinity probe based on CE or DBZ (**21a**–**e** and **22a**–**e**) biotinylated similar ~20 kDa polypeptides. Instead, several biotinylated bands at ~30–50 kDa were detected (Figure 3, panel a). Because the molecular size of PS1 N-terminal fragment (NTF) is ~30 kDa, we probed these fractions with anti-PS1 antibodies. Strikingly, PS1 NTF, but not CTF, was recovered in these fractions (Figure 3, panel b). The biotinylation of this 30 kDa band by **21c** and **22c**, named CE-BpB3 and DBZ-BpB3, respectively, was completely abolished by preincubation with the parental compounds (Figure 3, panel d, double asterisks). Moreover, no other known γ-secretase components (*i.e.*, nicastrin, Aph-1, Pen-2) (*1*) were detected in the fraction irradiated with the photoaffinity ligands (Y.T., T.I., T.T., data not shown). The biotinylation of the 30 kDa band was diminished in cell lysates from $PS1^{-/-}/PS2^{-/-}$ double knockout cells (MEF DKO), suggesting that CE and DBZ directly target PS1 NTF, different from DAPT that binds PS1 CTF (Figure 4, panel a).

To date, there is no report focusing on the pharmacological difference between DAPT and CE/DBZ on γ-secretase activity besides their potencies. However, it has been reported that all dipeptidics caused the accumulation of Aβ46 peptide, an intermediate fragment of γ-secretase cleavage in cells (*41*). Notably, this effect by DAPT was reversible, whereas CE/DBZ caused an irreversible Aβ46 accumulation, suggesting that the molecular mechanisms of DAPT and CE/DBZ on γ-secretase are enzymologically similar, but different. To gain insights into the molecular mechanism of inhibition by CE/DBZ as well as its binding region within PS1 NTF, we performed a competition assay of labeling by CE-BpB3 (Figure 5, panel a). Pharmacological and biochemical analyses suggest that γ-secretase harbors an "initial substrate binding site" that is distinct from the catalytic site (*1*). A transition-state analogue (*i.e.*, L-685,458) and aminoisobutyric acid-containing helical peptide-type inhibitors directly target the catalytic and substrate binding sites, respectively. Previously, we found that the labeling of PS1 CTF by DAP-BpB was displaced not only by CE/DBZ but also by L-685,458 and the helical peptide at higher concentrations (*13*). Similarly, the labeling of PS1 NTF by CE-BpB3 was completely abolished by preincubation with CE/DBZ and DAPT, while the target regions in PS1 are different (*i.e.*, NTF and CTF) (Figure 5, panel a). Thus, these dipeptidics might share the same binding space located at a broad molecular surface on PS1, or allosterically affect the structure of binding sites on PS1 NTF and CTF for CE/DBZ or DAPT, respectively. Moreover, L-685,458 weakly diminished the labeling of PS1 NTF by CE-BpB3 in a similar manner to that by DAP-BpB (Figure 5, panel b), consistent with the result of

the previous displacement experiments (*14*–*16*). Unexpectedly, however, the helical peptide (pep11) augmented the labeling of PS1 NTF by CE-BpB3 (Figure 5, panel b). Thus, like DAPT, the CE/DBZ binding site in PS1 might be distinct from either the catalytic site or the substrate binding site, although the substrate binding site occupancy by the helical peptide caused a structural effect on CE/DBZ binding site to increase the affinity for the compounds (*i.e.*, an open conformation). Collectively, these results suggest that the CE/DBZ binding site is functionally overlapping with the DAPT binding site, but the occupying chemical space in PS1 would be different. The C-terminal structure of these compounds might determine the final target region in PS1 and the mode of the actions on γ-secretase activity.

TABLE 2. Divergent synthesis of multifunctional molecular probes and their inhibitory potencies against *in vitro* Aβ40 generation

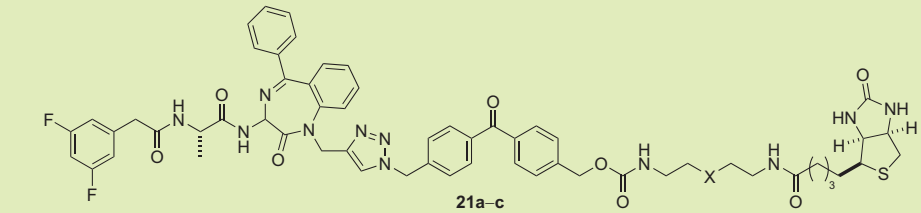

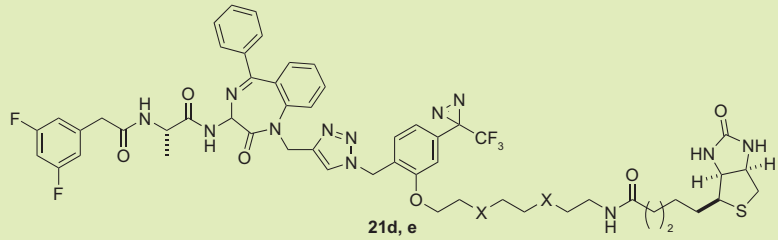

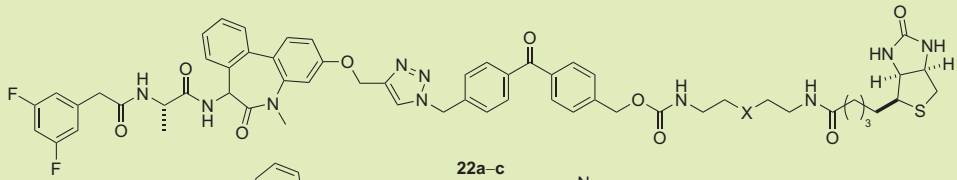

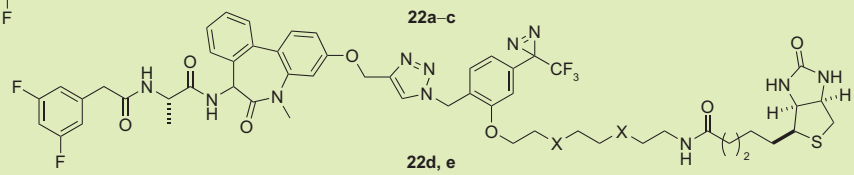

Product		% yield	IC_{50} (nM)
CE **(1)**			0.40
	21a: X = CH_2	89,[a] 92[b]	1.90
	21b: X = OCH_2CH_2O	88,[a] 65[b]	1.98
	21c: X = $(CH_2)_6$	83,[a] 89[b]	1.54
	21d: X = CH_2	85,[a] 68[b]	0.21
	21e: X = O	82,[a] 97[b]	1.18
DBZ **(2)**			0.75
	22a: X = CH_2	90,[a] 96[b]	0.063
	22b: X = OCH_2CH_2O	73,[a] 93[b]	1.91
	22c: X = $(CH_2)_6$	83,[a] 85[b]	1.43
	22d: X = CH_2	80[a]	0.14
	22e: X = O	84[a]	0.060

[a] $CuSO_4$ (0.1 equiv), sodium ascorbate (0.4 equiv), **20** (0.4 equiv), MeOH/H_2O (3:1), RT. [b] CuI (0.3 equiv), *i*-Pr_2NEt (10 equiv), MeOH, RT.

The labeling competition analysis revealed that the 45 kDa peptide was specifically biotinylated by CE- and DBZ-based photoaffinity probes (Figure 3, panels b and c), while the other biotinylated bands and smearing substances at higher molecular weight ranges were nonspecific. It was reported that LY411575 cross-inhibited the endoproteolytic activity of SPP, which shows molecular sizes of 45 and 90 kDa in monomeric and dimeric forms on SDS-PAGE, respectively (*9*–*11, 42, 43*). In fact, luciferase assay using ATF6-based substrate revealed that DBZ (ED_{50} = ~10 μM) as well as CE were able to inhibit SPP activity, albeit very low inhibitory potency in CE (18% inhibition at 100 μM) (see Supporting Information). However,

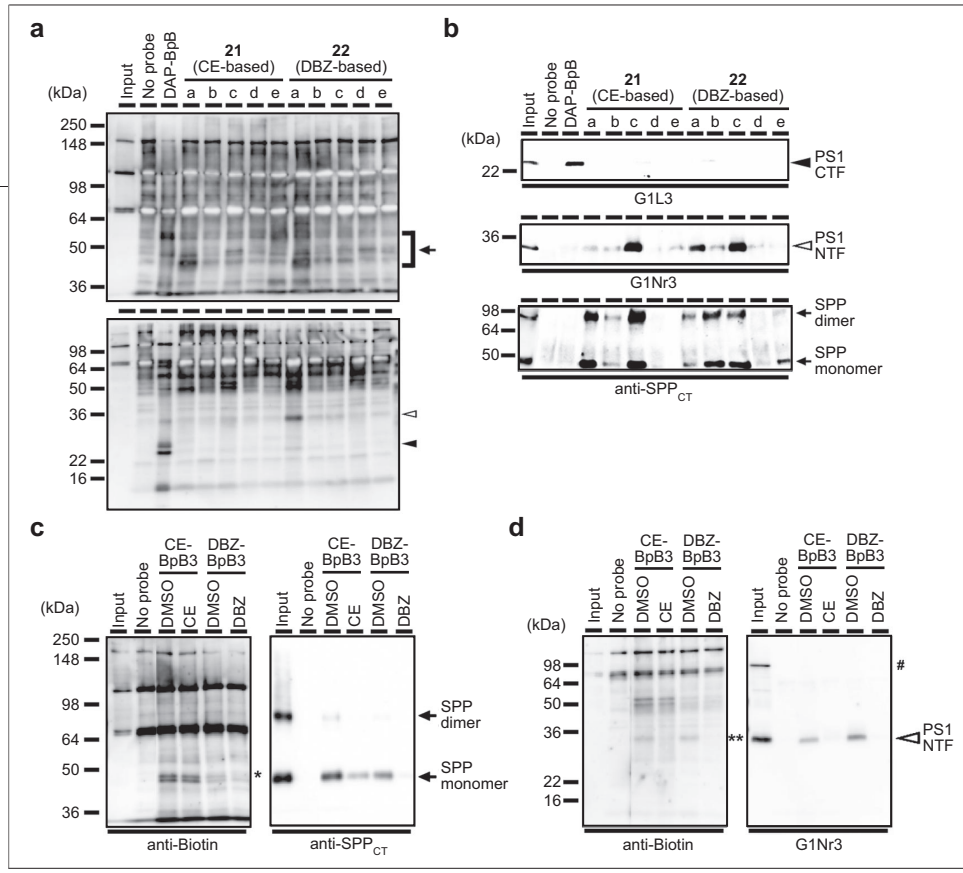

Figure 3. Immunoblot analysis of photoadducts labeled by CE- and DBZ-based probes. a) Biotinylated proteins were separated by 7.5% (upper) and 12.5% (lower) tris-glycine gels and probed with an antibiotin antibody. The arrow, the white arrowhead, and the black arrowhead indicate 45, 30, and 22 kDa biotinylated photoadducts, respectively. b) CE- and DBZ-based photoaffinity probes specifically target PS1 NTF (white arrowhead) and SPP (arrows). c and d) Labeling competition analysis. Samples were preincubated with parental compounds (1 μM) before addition of photoligands (10 nM) (CE-BpB3: 21c, DBZ-BpB3: 22c), and analyzed by 7.5% (c) and 12.5% (d) tris-glycine gels. The asterisk and the double asterisks denote the specifically labeled bands by the photoprobes. The arrows and the white arrowhead indicate SPP and PS1 NTF, respectively. The number sign denotes a nonspecific band. Photoadducts were probed using specific antibodies indicated below the gels. The appearance of the SPP dimer is dependent on the detergent and the treatment of SDS-PAGE samples as previously described (*48*).

DAPT never inhibited the SPP activity even at 100 μM as reported (*10, 11*). Thus, we explored the possibility that CE- as well as DBZ-based photoprobes target SPP. Immunoblot analysis using anti-SPP antibody revealed that SPP monomer and dimer were recovered in the irradiated fractions with CE-and DBZ-based photoprobes (Figure 3, panel c). The biotinylation of SPP was abolished by the parental compounds in a similar manner to that of PS1 NTF. Intriguingly, DAP-BpB never pulled down SPP in the irradiated fraction. Moreover, biotinylated SPP was observed in MEF DKO cell lysates, suggesting that the targeting of these photoprobes to SPP is totally independent of the existence of the γ-secretase complex (Figure 4, panel a). Finally, the specific labeling of the recombinant SPP polypeptide expressed in Sf9 cells by DBZ-BpB3 was obtained (Figure 4, panel b). Thus, consistent with the pharmacological potencies, CE and DBZ directly and specifically target SPP, in addition to γ-secretase.

Finally, we conducted a labeling competition assay using the dipeptidic compounds against SPP (*i.e.*, CE, DBZ, and DAPT) (Figure 5, panel c). The biotinylation of SPP by CE-BpB3 was unaffected by preincubation with DAPT, while CE and DBZ abolished the labeling, suggesting the specific binding of DAPT to γ-secretase. Consistent with our result, it was reported that the photoaffinity labeling of SPP using a transition-state analogue-based photoprobe was displaced by LY411575, but not DAPT (at 100 μM) (*9*), while DAPT competes for the binding of transition-state analogue to the γ-secretase complex (*13*). Moreover, NVP-AHW700-NX, the L-685,458 derivative that harbors the benzodiazepine moiety at C terminus, showed stronger potency against SPP than γ-secretase activity *in vitro* (*9*). Taken together, these data suggest that a bulky caprolactam moiety is involved in the stable binding of these dipeptidic compounds to SPP.

Here we propose a speculative view on the mode of binding of the dipeptidic compounds to PS1 (Figure 5, panel d). PS1 polypeptide within the γ-secretase complex harbors a binding pocket for the dipeptidic-type GSI that is composed of three functional sites: difluorobenzene, phenylglycine (Phg)-O*t*Bu, and caprolactam binding sites. Phg-O*t*Bu and caprolactam binding sites reside on PS1 CTF and PS1 NTF, respectively. In contrast, SPP has a binding pocket for the dipeptidic GSI formed only by the caprolactam binding site. Dipeptidic inhibitors initially bind to the difluorobenzene binding site in PS1 through their N terminus. Subsequently, the compounds target the secondary site, forming a stable complex with the enzyme *via* their C terminus, eventually inhibiting the proteolytic activity. The preference for the secondary binding site might be determined by the bulkiness of the C-terminal region of the compounds. Thus, DAPT and CE/DBZ target PS1 CTF and NTF, respec-

tively, by means of the structural preference and inhibit the γ-secretase activity. On the basis of this model, we speculate that DAPT and CE/DBZ would compete for the labeling of PS1 NTF and CTF, respectively, especially for binding to the primary difluorobenzene-binding site. CE/DBZ also forms a stable complex with SPP through its binding site in which bulky moiety is favored for association. In contrast, DAPT is unable to inhibit the SPP activity, because SPP lacks the structure corresponding to the difluorobenzene and/or Phg-O*t*Bu binding sites. Collectively, the structural variations of the C-terminal region of dipeptidic compounds might determine the mode of binding to PS1 or SPP, as well as the enzyme specificity of these inhibitors. However, photo-cross-linking and displacement experiments using affinity ligands do not allow a final conclusion as to the nature of the binding site(s) and the mode of action(s), because we cannot exclude the possibility of an allosteric effect caused by the affinity ligands. Further attempts to identify the binding sites using reconstituted enzyme and tandem mass spectrometry are currently underway. Ultimately, a high-dimensional structural analysis of γ-secretase coupled with GSI would be required to resolve this issue. Nonetheless, our photoaffinity labeling-based study has successfully culminated in the identification of the molecular targets of dipeptidic GSIs.

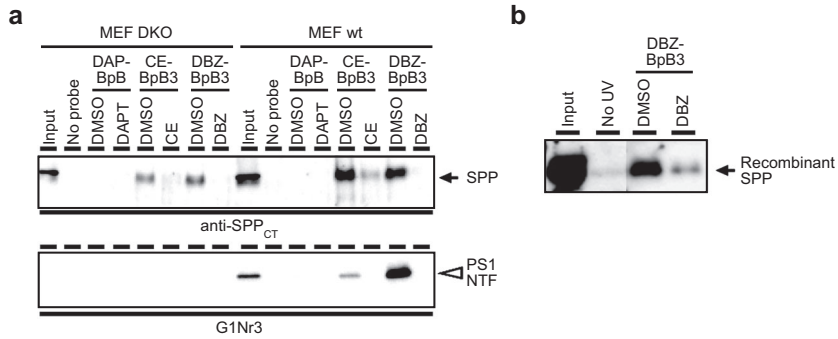

Figure 4. Specific labeling of SPP by CE- and DBZ-based photoprobes. a) Photoaffinity labeling experiment using MEF cells lacking PS or wild-type (MEF DKO and wt, respectively). The arrow and the white arrowhead indicate SPP and PS1 NTF, respectively. b) Photoaffinity labeling of recombinant SPP expressed in baculovirus-infected Sf9 cells by DBZ-BpB3 (22c).

Importantly, we found that the labeling ability and inhibitory potency of the multifunctional molecular probes

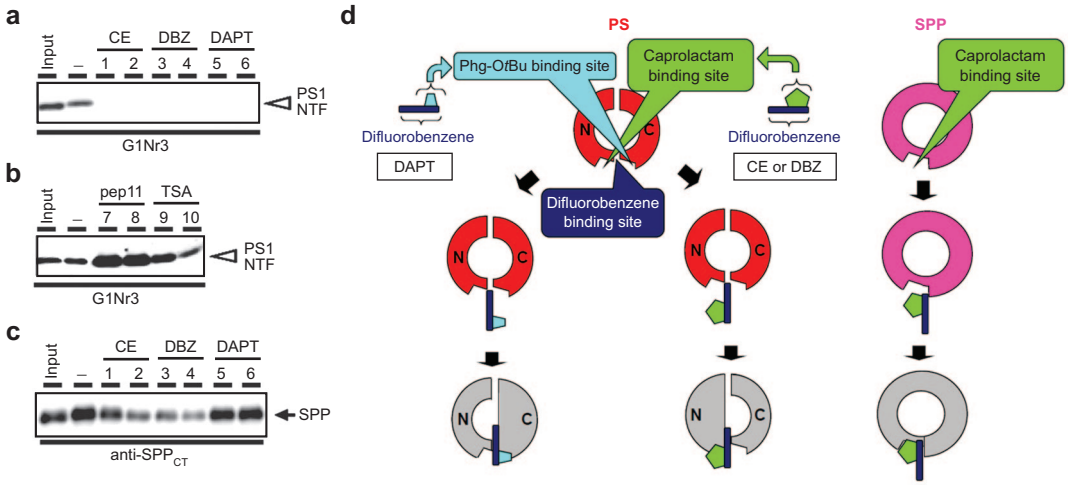

Figure 5. a–c) Competition assay against the labeling by CE-BpB3 (21c) in the presence of structurally different types of γ-secretase inhibitors. a and c) dipeptidics (CE, DBZ, DAPT), b) the helical peptide (pep11) and the transition-state analogue-type inhibitors (L-685,458). Concentrations of inhibitors are as follows: 1, 3, and 9: 10 nM; 2, 4, and 10: 100 nm; 5: 0.5 μM; 6 and 7: 5 μM; and 8: 50 μM. Antibodies used are shown under the panels. The white arrowheads and the arrow indicate PS1 NTF and SPP, respectively. d) Binding mode of dipeptidic inhibitors on GxGD-type intramembrane proteases (PS1/γ-secretase in red, SPP in purple). Both PS1 and SPP have a structurally similar caprolactam (green) binding site, whereas PS1 has a difluorobenzene (dark blue) and Phg-O*t*Bu binding site (sky blue). Enzymatic activities are inhibited by the formation of stable complex with the compounds (gray).

(**21a**–**e** and **22a**–**e**) do not necessarily correlate with each other, as reported (*44*), based on the following observations: photoaffinity probes with longer alkyl chain (*e.g.*, **21c** and **22c**) strongly labeled PS1-NTF and SPP but the inhibitory potency of these probes was comparable to those of other probes; benzophenone probes with ethylene glycol linker (**21b** and **22b**) and phenyl diazirine probes (**21d**,**e** and **22d**,**e**) were ineffective in our labeling experiments despite their robust inhibitory activities. Recently, we also observed the noncorrelation between the labeling ability and inhibitory potency in the analysis of DAP-BpB derivatives (*45*). Moreover, the inhibitory potency of CE against SPP activity was quite low, while the labeling potencies of CE-BpB3 and DBZ-BpB3 were almost similar within the concentration range we examined. These results might have been caused by the availability of reactive groups of the target enzyme close to the photoactivatable group. Moreover, the linker length and flexibility may affect the ability of the biotin moiety in the photoadducts to be captured by the streptavidin beads and the detection on immunoblots. Thus, these data illustrate the difficulties in the "rational" design of an effective multifunctional molecular probe, even if information about SARs of an affinity ligand moiety is sufficiently provided. However, at the same time, this underscores the significance of our diversity-based strategy as a means to discover an effective molecular probe. Together with the screening of novel compounds (*46*) and fine studies on the structure–mode of action relationships of several GSIs and their derivatives (*45, 47*), "integrated" chemical biological analyses would enable elucidation of the mode of action of the compounds as well as the molecular mechanism of the enzyme function.

CONCLUSIONS

Divergent synthesis of multifunctional molecular probes based on caprolactam-type dipeptidic GSIs, CE and DBZ, has been accomplished by means of the copper(I)-mediated azide/alkyne fusion process. Our strategy realized rapid and efficient generation of a diverse set of molecular probes harboring different types of photophore and linker units. Our photoaffinity labeling experiments provided direct evidence that, in sharp contrast to DAPT, CE and DBZ are specifically bound to both PS1-NTF and SPP. This is the first evidence indicating that dipeptidic GSI directly targets SPP. Our findings suggest that the structural difference between caprolactam-derived dipeptidic GSIs and DAPT causes differences not only in potency but also in biological mode of action, for example, enzyme selectivity. Our findings provide novel mechanistic insights into the actions of GSIs on PS-type intramembrane proteases, as well as a clue to the development of AD therapeutics targeting γ-secretase. We also found that the potency and labeling ability of photoaffinity probes do not necessarily correlate with each other. Thus, we emphasize here the advantage of our diversity-based strategy in the discovery of highly effective photoaffinity probes.

METHODS

Biological Activity and Photoaffinity Labeling Studies. HeLa, MEF wild-type (wt), DKO, and Sf9 cell lines were cultured, and their membrane fractions were collected as described (*13, 40, 45–50*). *In vitro* γ-secretase assay and measurement of Aβ by sandwich enzyme-linked immunosorbent assay (ELISA) were performed as described previously (*39*). Generation of recombinant baculovirus for human SPP will be described elsewhere. The synthetic process of DAPT and DAP-BpB was described previously (*21, 22*). CE, L-685,458, and pep11 were purchased from Calbiochem, Bachem, and Ito Lifescience, respectively. Photoaffinity labeling was performed as previously described with some modifications (*13*). Briefly, the solubilized cell membrane fraction was incubated with 10 or 100 nM photoaffinity compounds at 4 °C. In competition experiments, samples were prepared in the presence of other compounds with indicated concentrations based on each IC_{50} value as determined by *in vitro* γ-secretase assay, 40 min prior to the addition of photoaffinity ligands. The samples were irradiated on ice for 40 min using a B100A lamp (UVP) at a distance of 7 cm. The labeled samples were incubated with Dynabeads M-280 (Invitrogen) overnight at 4 °C and eluted from the resin by boiling for 1 min in the sample buffer. The labeled proteins were detected by SDS-PAGE/immunoblotting using antibodies. The rabbit polyclonal antibodies anti-PS1 NTF (G1Nr3) and CTF (G1L3), anti-SPP_{CT} were used as described before (*10, 42, 48, 50*). Anti-biotin rabbit polyclonal antibody was purchased from Bethyl.

Acknowledgment: We thank B. De Strooper (Katholieke Universiteit Leuven), A. Nyborg, T. Golde (Mayo Clinic), and K. Mori (Kyoto University) for valuable materials. This work is supported in part by Scientific Research on Priority Areas "Research on Pathomechanisms of Brain Disorders", "Creation of Biologically Functional Molecules", and the 21st century COE program from the Ministry of Education, Culture, Sports, Science and Technology and by the Program for Promotion of Fundamental Studies in Health Sciences of the National Institute of Biomedical Innovation, Japan. We are also grateful to Takeda Pharmaceutical Co. for Aβ ELISA and our current/previous lab members for helpful discussions and technical assistance. H.F. and Y.T. were a postdoctoral fellow and a research fellow of the Japan Society for the Promotion of Science, respectively.

Supporting Information Available: This material is available free of charge *via* the Internet.

REFERENCES

1. Tomita, T., and Iwatsubo, T. (2006) γ-Secretase as a therapeutic target for treatment of Alzheimer's disease, *Curr. Pharm. Des. 12*, 661–670.
2. Roy, M, Pear, W.S., and Aster, J.C. (2007) The multifaceted role of notch in cancer, *Curr. Opin. Genet. Dev. 17*, 52–59.
3. Weihofen, A., Binns, K., Lemberg, M.K., Ashman, K., and Martoglio, B. (2002) Identification of signal peptide peptidase, a presenilin-type aspartic protease, *Science 296*, 2215–2218.
4. Grigorenko, A. P., Moliaka, Y. K., Soto, M. C., Mello, C. C., and Rogaev, E. I. (2004) The *Caenorhabditis elegans* IMPAS gene, *imp-2*, is essential for development and is functionally distinct from related presenilins, *Proc. Natl. Acad. Sci. U.S.A. 101*, 14955–14960.
5. Casso, D. J., Tanda, S., Biehs, B., Martoglio, B., and Kornberg, T. B. (2005) *Drosophila* signal peptide peptidase is an essential protease for larval development, *Genetic 170*, 139–148.
6. Krawitz, P., Haffner, C., Fluhrer, R., Steiner, H., Schmid, B., and Haass, C. (2005) Differential localization and identification of a critical aspartate suggest non-redundant proteolytic functions of the presenilin homologues SPPL2b and SPPL3, *J. Biol. Chem. 280*, 39515–39523.
7. Friedmann, E., Hauben, E., Maylandt, K., Schleeger, S., Vreugde, S., Lichtenthaler, S. F., Kuhn, P. H., Stauffer, D., Rovelli, G., and Martoglio, B. (2006) SPPL2a and SPPL2b promote intramembrane proteolysis of TNFα in activated dendritic cells to trigger IL-12 production, *Nat. Cell Biol. 8*, 843–848.
8. McLauchlan, J., Lemberg, M. K., Hope, G., and Martoglio, B. (2002) Intramembrane proteolysis promotes trafficking of hepatitis C virus core protein to lipid droplets, *EMBO J. 21*, 3980–3988.
9. Weihofen, A., Lemberg, M. K., Friedmann, E., Rueeger, H., Schmitz, A., Paganetti, P., Rovelli, G., and Martoglio, B. (2003) Targeting presenilin type aspartic protease signal peptide peptidase with γ-secretase inhibitors, *J. Biol. Chem. 278*, 16528–16533.
10. Nyborg, A. C., Jansen, K., Ladd, T. B., Fauq, A., and Golde, T. E. (2004) A signal peptide peptidase (SPP) reporter activity assay based on the cleavage of type II membrane protein substrates provides further evidence for an inverted orientation of the SPP active site relative to presenilin, *J. Biol. Chem. 279*, 43148–43156.
11. Dev, K. K., Chatterjee, S., Osinde, M., Stauffer, D., Morgan, H., Kobialko, M., Dengler, U., Rueeger, H., Martoglio, B., and Rovelli, G. (2006) Signal peptide peptidase dependent cleavage of type II transmembrane substrates releases intracellular and extracellular signals, *Eur J Pharmacol. 540*, 10–17.
12. Seiffert, D., Bradley, J. D., Rominger, C. M., Rominger, D. H., Yang, F., Meredith, J. E., Jr., Wang, Q., Roach, A. H., Thompson, L. A., Spitz, S. M., Higaki, J. N., Prakash, S. R., Combs, A. P., Copeland, R. A., Arneric, S. P., Hartig, P. R., Robertson, D. W., Cordell, B., Stern, A. M., Olson, R. E., and Zaczek, R. (2000) Presenilin-1 and -2 are molecular targets for γ-secretase inhibitors, *J. Biol. Chem. 275*, 34086–34091.
13. Morohashi, Y., Kan, T., Tominari, Y., Fuwa, H., Okamura, Y., Watanabe, N., Sato, C., Natsugari, H., Fukuyama, T., Iwatsubo, T., and Tomita, T. (2006) Carboxyl-terminal fragment of presenilin is the molecular target of γ-secretase-specific dipeptidic inhibitor DAPT (*N*-[*N*-(3,5-difluorophenacetyl)-L-alanyl]-*S*-phenylglycine *t*-butyl ester), *J. Biol. Chem. 281*, 14670–14676.
14. Tian, G., Sobotka-Briner, C. D., Zysk, J., Liu, X., Birr, C., Sylvester, M. A., Edwards, P. D., Scott, C. D., and Greenberg, B. D. (2002) Linear non-competitive inhibition of solubilized human γ-secretase by pepstatin A methylester, L685458, sulfonamides, and benzodiazepines, *J. Biol. Chem. 277*, 31499–31505.
15. Tian, G., Ghanekar, S. V., Aharony, D., Shenvi, A. B., Jacobs, R. T., Liu, X., and Greenberg, B. D. (2003) The mechanism of γ-secretase: multiple inhibitor binding sites for transition state analogs and small molecule inhibitors, *J. Biol. Chem. 278*, 28968–28975.
16. Clarke, E. E., Churcher, I., Ellis, S., Wrigley, J. D., Lewis, H. D., Harrison, T., Shearman, M. S., and Beher, D. (2006) Intra- or intercomplex binding to the γ-secretase enzyme. a model to differentiate inhibitor classes, *J. Biol. Chem. 281*, 31279–31289.
17. Hofmann, K., and Kiso, Y. (1976) An approach to the targeted attachment of peptides and proteins to solid supports, *Proc. Natl. Acad. Sci. U.S.A. 73*, 3516–3518.
18. Dormán, G., and Prestwich, G. D. (1994) Benzophenone photophores in biochemistry, *Biochemistry 33*, 5661–5673.
19. Kotzyba-Hibert, F., Kapfer, I., and Goeldner, M. (1995) Recent trends in photoaffinity-labeling, *Angew. Chem., Int. Ed. Engl. 34*, 1296–1312.
20. Dormán, G., and Prestwich, G. D. (2000) Using photolabile ligands in drug discovery and development, *Trends Biotechnol. 18*, 64–77.
21. Kan, T., Tominari, Y., Morohashi, Y., Natsugari, H., Tomita, T., Iwatsubo, T., and Fukuyama, T. (2003) Solid-phase synthesis of photoaffinity probes. highly efficient incorporation of biotin-tag and cross-linking groups, *Chem. Commun. 17*, 2244–2245.
22. Kan, T., Tominari, Y., Rikimaru, K., Morohashi, Y., Natsugari, H., Tomita, T., Iwatsubo, T., and Fukuyama, T. (2004) Parallel synthesis of DAPT derivatives and their γ-secretase-inhibitory acitivity, *Bioorg. Med. Chem. Lett. 14*, 1983–1985.
23. Rostovtsev, V. V., Green, L. G., Fokin, V. V., and Sharpless, K. B. (2002) A stepwise Huisgen cycloaddition process: copper(I)-catalyzed regioselective "ligation" of azides and terminal alkynes, *Angew. Chem., Int. Ed. 41*, 2596–2599.
24. Tornøe, C. W., Christensen, C., and Meldal, M. (2002) Peptidotriazoles on solid phase: [1,2,3]-triazoles by regiospecific Cu(I)-catalyzed 1,3-dipolar cycloadditions of terminal alkynes to azides, *J. Org. Chem. 67*, 3057–3064.
25. Hatanaka, Y., Kempin, U., and Park, J.-J. (2000) One-step synthesis of biotinyl photoprobes from unprotected carbohydrates, *J. Org. Chem. 65*, 5639–5643.
26. Wang, J., Uttamchandani, M., Li, J., Hu, M., and Yao, S. Q. (2006) "Click" synthesis of small molecule probes for activity-based fingerprinting of matrix metalloproteases, *Chem. Commun.* 3783–3785.
27. Inverarity, I. A., and Hulme, A. N. (2007) Marked small molecule libraries: a truncated approach to molecular probe design, *Org. Biomol. Chem. 5*, 636–643.
28. Hashimoto, M., Hatanaka, Y., Yang, J., Dhesi, J., and Holman, G. D. (2001) Synthesis of biotinylated bis(D-glucose) derivatives for glucose transporter photoaffinity labeling, *Carbohydrate Res. 331*, 119–127.
29. Hashimoto, M., Kanaoka, Y., and Hatanaka, Y. (1997) A versatile approach for functionalization of 3-aryl-3-trifluoromethyldiazirine photophor, *Heterocycles 46*, 119–122.
30. Hatanaka, Y., Hashimoto, M., Kurihara, H., Nakayama, H., and Kanaoka, Y. (1994) Novel family of aromatic diazirines for photoaffinity-labeling, *J. Org. Chem. 59*, 383–387.
31. Egbertson, M. S., Chang, C. T.-C., Duggan, M. E., Gould, R. J., Halczenko, W., Hartman, G. D., Laswell, W. L., Lynch, J. J., Lynch, R. J., Manno, P. D., Naylor, A. M., Prugh, J. D., Ramjit, D. R., Sitko, G. R., Smith, R. S., Turchi, L. M., and Zhang, G. (1994) Non-peptide fibrinogen receptor antagonists. 2. optimization of a tyrosine template as a mimic for Arg-Gly-Asp, *J. Med. Chem. 37*, 2537–2551.
32. Hatanaka, Y., Hashimoto, M., and Kanaoka, Y. (1994) A novel biotinylated heterobifunctional cross-linking reagent bearing an aromatic diazirine, *Bioorg. Med. Chem. 2*, 1367–1373.
33. Fang, K., Hashimoto, M., Jockusch, S., Turro, N. J., and Nakanishi, K. (1998) A bifunctional photoaffinity probe for ligand/receptor interaction studies, *J. Am. Chem. Soc. 120*, 8543–8544.
34. Li, H. Y., Liu, Y., Fang, K., and Nakanishi, K. (1999) A simple photoaffinity-labeling protocol, *Chem. Commun.* 365–366.

35. Hashimoto, M., Okamoto, S., Nabeta, K., and Hatanaka, Y. (2004) Enzyme cleavable and biotinylated photoaffinity ligand with diazirine, *Bioorg. Med. Chem. Lett. 14*, 2447–2450.
36. Park, J.-J., Sadakane, Y., Masuda, K., Tomohiro, T., Nakano, T., and Hatanaka, Y. (2005) Synthesis of diazirinyl photoprobe carrying a novel cleavable biotin, *ChemBioChem 6*, 814–818.
37. Butcher, J. W., Liverton, N. J., Selnick, H. G., Elliot, J. M., Smith, G. R., Tebben, A. J., Pribush, D. A., Wai, J. S., and Claremon, D. A. (1996) Preparation of 3-amino-1,4-benzodiazepin-2-ones via direct azidation with trisyl azide, *Tetrahedron Lett. 37*, 6685–6688.
38. Fuwa, H., Okamura, Y., Morohashi, Y., Tomita, T., Iwatsubo, T., Kan, T., Fukuyama, T., and Natsugari, H. (2004) Highly efficient synthesis of medium-sized ring lactams via Staudinger-Aza-Wittig reaction of ω-azido pentafluorophenyl ester: synthesis and biological evaluation of LY411575 analogues, *Tetrahedron Lett. 45*, 2323–2326.
39. Wang, Q., Chan, T. R., Hilgraf, R., Fokin, V. V., Sharpless, K. B., and Finn, M. G. (2003) Bioconjugation by copper(I)-catalyzed azide-alkyne [3+2] cycloaddition, *J. Am. Chem. Soc. 125*, 3192–3193.
40. Takahashi, Y., Hayashi, I., Tominari, Y., Rikimaru, K., Morohashi, Y., Kan, T., Natsugari, H., Fukuyama, T., Tomita, T., and Iwatsubo, T. (2003) Sulindac sulfide is a noncompetitive γ-secretase inhibitor that preferentially reduces Aβ42 generation, *J. Biol. Chem. 278*, 18664–18670.
41. Zhao, G., Tan, J., Mao, G., Cui, M. Z., and Xu, X. (2007) The same γ-secretase accounts for the multiple intramembrane cleavages of APP, *J. Neurochem. 100*, 1234–1246.
42. Nyborg, A. C., Kornilova, A. Y., Jansen, K., Ladd, T. B., Wolfe, M. S., and Golde, T. E. (2004) Signal peptide peptidase forms a homodimer that is labeled by an active site-directed γ-secretase inhibitor, *J. Biol. Chem. 279*, 15153–15160.
43. Nyborg, A. C., Ladd, T. B., Jansen, K., Kukar, T., and Golde, T. E. (2006) Intramembrane proteolytic cleavage by human signal peptide peptidase like 3 and malaria signal peptide peptidase, *FASEB J. 20*, 1671–1679.
44. Fujii, T., Manabe, Y., Sugimoto, T., and Ueda, M. (2005) Detection of 210 kDa receptor protein for a leaf-movement factor by using novel photoaffinity probes, *Tetrahedron 61*, 7874–7893.
45. Kan, T., Kita, Y., Morohashi, Y., Tominari, Y., Hosoda, S., Tomita, T., Natsugari, H., Iwatsubo, T., and Fukuyama, T. (2007) Convenient synthesis of photoaffinity probes and evaluation of their abilities, *Org. Lett. 9*, 2055–2058.
46. Takahashi, Y., Fuwa, H., Kaneko, A., Sasaki, M., Yokoshima, S., Koizumi, H., Takebe, T., Kan, T., Iwatsubo, T., Tomita, T., Natsugari, H., and Fukuyama, T. (2006) Novel γ-secretase inhibitors discovered by library screening of in-house synthetic natural product intermediates, *Bioorg. Med. Chem. Lett. 16*, 3813–3816.
47. Fuwa, H., Hiromoto, K., Takahashi, Y., Yokoshima, S., Kan, T., Fukuyama, T., Iwatsubo, T., Tomita, T., and Natsugari, H. (2006) Synthesis of biotinylated photoaffinity probes based on arylsulfonamide γ-secretase inhibitors, *Bioorg. Med. Chem. Lett. 16*, 4184–4189.
48. Tomita, T., Takikawa, R., Koyama, A., Morohashi, Y., Takasugi, N., Saido, T. C., Maruyama, K., and Iwatsubo, T. (1999) C Terminus of presenilin is required for overproduction of amyloidogenic Aβ42 through stabilization and endoproteolysis of presenilin, *J. Neurosci. 19*, 10627–10634.
49. Hayashi, I., Urano, Y., Fukuda, R., Isoo, N., Kodama, T., Hamakubo, T., Tomita, T., and Iwatsubo, T. (2004) Selective reconstitution and recovery of functional γ-secretase complex on budded baculovirus particles, *J. Biol. Chem. 279*, 38040–38046.
50. Ogura, T., Mio, K., Hayashi, I., Miyashita, H., Fukuda, R., Kopan, R., Kodama, T., Hamakubo, T., Iwatsubo, T., Tomita, T., and Sato, C. (2006) Three-dimensional structure of the γ-secretase complex, *Biochem. Biophys. Res. Commun. 343*, 525–534.